

Optimal projection in a Koopman-based sorting-free Hill method

Fabia Bayer and Remco I. Leine

Institute for Nonlinear Mechanics, University of Stuttgart, Germany,
{bayer, leine}@inm.uni-stuttgart.de,
www.inm.uni-stuttgart.de

Abstract. In this work, a novel method to determine the stability of periodic solutions is demonstrated. Using the Koopman framework, the linear time-periodic nonautonomous perturbed dynamics around a periodic solution can be approximated by a linear autonomous system of higher order, whose system matrix is the well-known Hill matrix. Evaluation of the closed form solution reveals that the monodromy matrix can be approximated by the Hill matrix, using only a matrix exponential and a projection instead of solving a large eigenvalue problem or integrating numerically over one period. There does not exist a unique choice for the projection of the Hill matrix to the monodromy matrix, and various ways to obtain a suitable projection are discussed in this paper. The performance of the novel method is illustrated for the vertically excited multiple pendulum.

Keywords: Floquet multipliers, Floquet exponents, periodic solutions, stability, monodromy matrix

1 Introduction

The numerical characterization of periodic solutions in nonlinear systems and their stability is a task of greatest interest in engineering application, e.g. for nonlinear vibration analysis in structural dynamics. One common approach to find these periodic solutions is the frequency-based Harmonic Balance method (HBM) [1]. The HBM by itself does not yield the stability information necessary to detect bifurcations (e.g. period-doubling and Neimark-Sacker bifurcations). The Hill method is often employed in combination with the HBM to obtain stability information. In the Hill method, the Hill matrix is constructed (sometimes as a by-product of an HBM based continuation method). Its eigenvalues approximate the Floquet exponents, thereby giving stability information [2, 3].

However, two critical problems make this Hill method often unattractive in practice. On the one hand, from a numerical viewpoint, computing the eigenvalues of the large Hill matrix is computationally expensive and potentially inaccurate [4]. On the other hand, only a nontrivial subset of these eigenvalues must be considered for correct assertion of stability. This process is known in the literature as *sorting* of Floquet exponent candidates. Determination of this subset

is area of ongoing research, with the approaches being based on the imaginary parts [2, 5] and potentially in addition the real parts [6] of the eigenvalues, or alternatively symmetry considerations of the eigenvectors [3].

Recently, the authors proposed a novel approach for obtaining stability information from the Hill matrix [7], using the Koopman framework to compute an approximation of the monodromy matrix directly (i.e. without computing a large number of eigenvalues and subsequent sorting). This method involves the action of the matrix exponential of the Hill matrix on a smaller sparse matrix, followed by a projection to the $n \times n$ monodromy matrix. The stability of the periodic solution can then be assessed directly from the n eigenvalues of the monodromy matrix, known to be the Floquet multipliers. The Koopman basis functions utilized in the considered approach yield multiple independent estimates of the considered perturbed state, and hence the projection from the linear autonomous Koopman lift to the monodromy matrix is not unique. In this paper, multiple approaches to choosing a suitable projection from the family of applicable candidates are discussed.

2 Classical Floquet theory

We consider linear time-periodic dynamical systems

$$\dot{\mathbf{y}}(t) = \mathbf{J}(t)\mathbf{y}(t), \quad \mathbf{J}(t) = \mathbf{J}(t + T), \quad \mathbf{y}(0) = \mathbf{y}_0 \in \mathbb{R}^n. \quad (1)$$

This system class results, in particular, if a perturbation of an (autonomous or non-autonomous) smooth nonlinear dynamical system around a T -periodic solution is linearized. Floquet's well-known theorem (see, e.g., [8]) states that solutions of (1) can be expressed using the fundamental solution matrix by

$$\mathbf{y}(t) = \mathbf{\Phi}(t)\mathbf{y}_0 = \mathbf{P}(t)e^{\mathbf{Q}t}\mathbf{y}_0, \quad (2)$$

where the matrix $\mathbf{Q} \in \mathbb{C}^{n \times n}$ is constant and describes the long-term behavior, while the matrix $\mathbf{P}(t) \in \mathbb{C}^{n \times n}$ is T -periodic with $\mathbf{P}(0) = \mathbf{I}$ and describes the oscillatory effects within each period. The formulation (2) leads to two equivalent stability criteria:

- The monodromy matrix $\mathbf{\Phi}_T := \mathbf{\Phi}(T)$, whose eigenvalues $\{\lambda_l\}_{l=1}^n$ are called Floquet multipliers (FM), defines a discrete map $\mathbf{y}_k \mapsto \mathbf{\Phi}_T\mathbf{y}_k = \mathbf{y}(t_k + T)$ that evolves the perturbed state one period at a time. This means that (1) is asymptotically stable if all FM lie within the unit circle in the complex plane and unstable if at least one FM lies outside.
- As the matrix \mathbf{P} in (2) is periodic and can therefore neither vanish nor grow unbounded, the longterm behavior of the solution is governed by $e^{\mathbf{Q}t}$. Consequently, if all eigenvalues $\{\alpha_l\}_{l=1}^n = \text{eig}(\mathbf{Q})$ of \mathbf{Q} , also called Floquet exponents (FE), have a real part smaller than zero, the system (1) is asymptotically stable and if one FE has a real part larger than zero, it is unstable.

With $\Phi_T = e^{\mathbf{Q}T}$, the Floquet exponents and the Floquet multipliers can be transformed into each other via $\lambda_l = e^{\alpha_l T}$.

The system matrix \mathbf{J} has a Fourier series $\mathbf{J}(t) = \sum_{k=-\infty}^{\infty} \mathbf{J}_k e^{ik\omega t}$ with $\omega = \frac{2\pi}{T}$. Arranged in a block-Toeplitz structure, these Fourier coefficients make up the infinite-dimensional Hill matrix, also called the harmonic state operator. Its spectrum is constituted by the FE of the system (1) [5]. However, when utilized numerically, it must be truncated to a finite order $N_{\mathbf{u}}$ by

$$\mathbf{H} = \begin{pmatrix} \mathbf{J}_0 + iN_{\mathbf{u}}\omega\mathbf{I} & \dots & \mathbf{J}_{-2N_{\mathbf{u}}} \\ \vdots & \ddots & \vdots \\ \mathbf{J}_{2N_{\mathbf{u}}} & \dots & \mathbf{J}_0 - iN_{\mathbf{u}}\omega\mathbf{I} \end{pmatrix}, \quad (3)$$

incurring truncation errors in its eigenvalues. Usually, these errors are dealt with by selecting a subset of the eigenvalues of \mathbf{H} based on one of various sorting criteria [5, 3, 6]. This work, in contrast, uses the Koopman framework to reinterpret the truncated Hill matrix as the system matrix of an autonomous linear system, allowing to obtain the FM from a closed form approximation of the monodromy matrix.

3 Koopman lifting the LTV dynamics

The Koopman framework allows to approximate a time-dependent nonlinear dynamical system by a linear and possibly autonomous system of arbitrary degree. For a deeper insight, the reader is referred to [7, 9] and the references therein.

For a nonlinear dynamical system $\dot{\mathbf{x}} = \mathbf{f}(\mathbf{x})$ (where \mathbf{f} can also describe a nonautonomous system in extended state-space form) and a function space \mathcal{F} of observables, the Koopman infinitesimal generator $L : \mathcal{F} \rightarrow \mathcal{F}$ maps an observable to its derivative along the flow, i.e. if $g \in \mathcal{F}$ then

$$(Lg)(\mathbf{x}) = \dot{g}(\mathbf{x}) = \frac{\partial g}{\partial \mathbf{x}} \mathbf{f}(\mathbf{x}). \quad (4)$$

This equivalent representation of the dynamical system is linear in its argument g , even if the original dynamics in state-space form was nonlinear. However, the linearity comes at the price of an infinite dimensional function space.

To make the approach numerically feasible, a projection to a finite-dimensional subspace $\mathcal{F}_N \subset \mathcal{F}$ spanned by the basis functions $\Psi := \{\Psi_1, \dots, \Psi_N\}$ is considered. Using an orthogonal projection, the derivative of the basis functions can be separated by $(L\Psi)(\mathbf{x}) = \dot{\Psi}(\mathbf{x}) =: \mathbf{A}\Psi(\mathbf{x}) + \mathbf{r}(\mathbf{x})$, where the constant matrix \mathbf{A} collects all linear coefficients for the portion of $\dot{\Psi}$ that lies in \mathcal{F}_N , and the elements in \mathbf{r} are orthogonal to \mathcal{F}_N . Using $\mathbf{z}(t) \approx \Psi(\mathbf{x}(t))$ and neglecting this orthogonal remainder, the corresponding lifted dynamics

$$\dot{\mathbf{z}} = \mathbf{A}\mathbf{z}; \quad \mathbf{z}(0) = \Psi(\mathbf{x}_0) \quad (5)$$

approximates the original dynamics.

The authors recently showed [7] that the dynamics (1) has a Koopman lift $\dot{\mathbf{z}} = \mathbf{H}\mathbf{z}$, where \mathbf{H} is the truncated Hill matrix (3) of order $N_{\mathbf{u}}$, if observables

$$\Psi_{\text{lin}}(\mathbf{y}, t) = (\mathbf{y}^T e^{iN_{\mathbf{u}}\omega t}, \dots, \mathbf{y}^T, \dots, \mathbf{y}^T e^{-iN_{\mathbf{u}}\omega t})^T \in \mathbb{C}^N \quad (6)$$

that are linear in the state and derived from Fourier basis functions in time are chosen as a basis. Expressing (5) using the basis Ψ_{lin} as a linear dynamical system with \mathbf{y} as output and \mathbf{y}_0 as initial condition, we obtain

$$\begin{aligned} \dot{\mathbf{z}}(t) &= \mathbf{H}\mathbf{z}(t) \\ \mathbf{y}(t) &\approx \mathbf{z}_{\mathbf{y}}(t) = \mathbf{C}(t)\mathbf{z}(t) \\ \mathbf{z}(0) &= \Psi_{\text{lin}}(\mathbf{y}(0), 0) = \mathbf{W}\mathbf{y}_0 \end{aligned} \quad (7)$$

as a dynamical systems interpretation of the Hill matrix. Here, $\mathbf{C}(t) \in \mathbb{C}^{n \times N}$ is a possibly time-dependent projection matrix that satisfies

$$\mathbf{C}(t)\Psi_{\text{lin}}(\mathbf{y}, t) = \mathbf{y} \quad \forall t \in [0, T] \quad (8)$$

and $\mathbf{W} \in \mathbb{C}^{N \times n}$ is a stack of $2N_{\mathbf{u}} + 1$ identity matrices. While there is a $nN_{\mathbf{u}}$ -parameter family of time-dependent admissible \mathbf{C} matrices, one option is to pick the entries in (6) that correspond to frequency zero. For this *naive* choice, the matrix \mathbf{C} is constant and given by

$$\mathbf{C}_0 = (\mathbf{0} \dots \mathbf{0} \mathbf{I}_{n \times n} \mathbf{0} \dots \mathbf{0}) . \quad (9)$$

4 Monodromy matrix and stability

As the system (7) is linear time-autonomous (possibly except for \mathbf{C}), its closed form solution can be explicitly computed as

$$\mathbf{y}(t) \approx \mathbf{z}_{\mathbf{y}}(t) = \mathbf{C}(t)e^{\mathbf{H}t}\mathbf{z}(0) = \mathbf{C}(t)e^{\mathbf{H}t}\mathbf{W}\mathbf{y}(0) . \quad (10)$$

The key finding of [7] is that the matrix $\mathbf{C}(t)e^{\mathbf{H}t}\mathbf{W} \in \mathbb{R}^{n \times n}$ is an approximation of the fundamental solution matrix $\Phi(t)$, which is the matrix that satisfies $\mathbf{y}(t) = \Phi(t)\mathbf{y}(0)$. In particular, for $t = T$, the monodromy matrix is approximated via

$$\Phi_T \approx \mathbf{C}(T)e^{\mathbf{H}T}\mathbf{W} . \quad (11)$$

Consequently, the Floquet multipliers can be approximated by the eigenvalues of (11). This constitutes a novel stability method arising from the Hill matrix, which we will name *projection-based Koopman-Hill stability method*. It is labeled *sorting-free* because the approach does not use the same steps as standard Hill stability methods [3, 6], as illustrated in Figure 1.

In all these state-of-the-art Hill method approaches, the complete set of eigenvalues of the Hill matrix are determined in the first step. This is a computationally intense operation which may lack accuracy. Only n of these $n(2N_{\mathbf{u}} + 1)$ eigenvalues approximate the true Floquet exponents, while the others do not carry

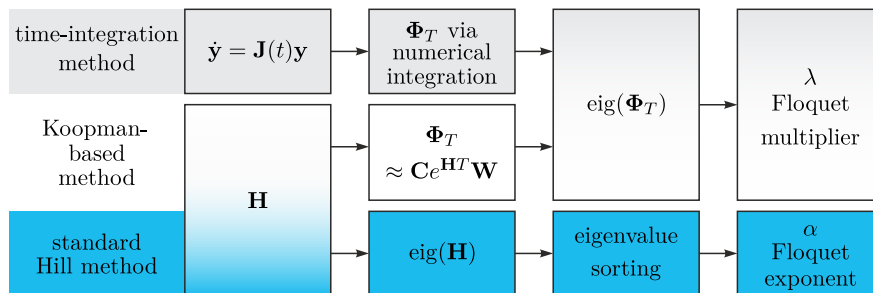


Fig. 1: Flowchart comparing the three general stability approaches. For each of the methods, the most computationally demanding step is located in the second column.

physical meaning and may compromise the stability information. The state-of-the-art methods differ in the sorting algorithms that are used to identify this subset.

In the proposed sorting-free method, however, once the Hill matrix is obtained, the monodromy matrix is determined directly via (11). As \mathbf{H} will be relatively sparse in many applications, the action of the matrix exponential on the smaller matrix \mathbf{W} can be determined efficiently [10]. As a second step in the sorting-free approach, it remains to solve $\text{eig}(\Phi_T)$. The real-valued Φ_T of size $n \times n$ is in general much smaller than the Hill matrix $\mathbf{H} \in \mathbb{C}^{n(2N_{\mathbf{u}}+1) \times n(2N_{\mathbf{u}}+1)}$. The result are n FM and no a posteriori sorting of candidates is necessary.

Alternatively, the monodromy matrix can be determined via time-integration of the LTV dynamics (1) over one period [4], commonly referred to as the $2n$ -pass method¹. Afterwards, it again remains to solve the eigenvalue problem on the $n \times n$ monodromy matrix. The presented sorting-free projection method therefore has the advantage of being a Hill-based method, which is favorable in an HBM setting, and at the same time only requiring to compute the smaller eigenvalue problem of the monodromy matrix, similar to the time-integration based method.

5 Projection matrix optimization

The aim of this section is to characterize the class of time-dependent matrices \mathbf{C} that satisfy the constraint (8) and yield approximations of the monodromy matrix via (11). The l -th row of (8) is expressed by $y_l = \sum_{k=-N_{\mathbf{u}}}^{N_{\mathbf{u}}} c_{l,k}(t)y_l e^{ik\omega t}$ as all y_l are independent. This equality can only hold if

$$c_{l,k}(t) = \hat{c}_{l,k} e^{-ik\omega t}, \quad \sum_{k=-N_{\mathbf{u}}}^{N_{\mathbf{u}}} \hat{c}_{l,k} = 1. \quad (12)$$

¹ The number n in the name $2n$ -pass refers to the number of DOF of the mechanical system, called n_p below, and should not be confused with the number of states n .

Further, the conjugate symmetry $\hat{c}_{l,k} = \bar{\hat{c}}_{l,-k}$ ensures real-valued results in the dynamics (7). Hence, $N_{\mathbf{u}}$ independent complex-valued parameters characterize admissible choices for the l -th row of \mathbf{C} , where all but $2N_{\mathbf{u}} + 1$ entries vanish.

It is sensible to collect all parameters $\hat{c}_{k,l}$ into a long row vector $\hat{\mathbf{c}}_{\text{all}}$ with $\hat{\mathbf{c}}_{\text{all}} = (\hat{c}_{1,-N_{\mathbf{u}}}, \dots, \hat{c}_{1,N_{\mathbf{u}}}, \hat{c}_{2,-N_{\mathbf{u}}}, \dots, \hat{c}_{n,N_{\mathbf{u}}})$. As a practicable condition, $\hat{\mathbf{c}}_{\text{all}}$ can be chosen such that the resulting fundamental matrix optimally satisfies the original dynamics. Substituting (11) into the dynamics (1) yields

$$\mathbf{R}(t, \hat{\mathbf{c}}_{\text{all}}) := (\mathbf{C}(t)e^{\mathbf{H}t}\mathbf{W})' - \mathbf{J}(t)\mathbf{C}(t)e^{\mathbf{H}t}\mathbf{W} \approx \dot{\Phi}(t) - \mathbf{J}(t)\Phi(t) = \mathbf{0} \quad (13)$$

and since this residual is ideally expected to vanish, a cost function can be defined via $L_{\text{var}}(\hat{\mathbf{c}}_{\text{all}}) = \int_0^T \|\mathbf{R}(t, \hat{\mathbf{c}}_{\text{all}})\|^2 dt$. The time-dependent matrix $\mathbf{C}_{\text{int}}(t)$ created from the $\hat{\mathbf{c}}_{\text{all}}$ that minimize this cost while satisfying the constraints (12) will produce a good estimate of the monodromy matrix.

The special structure of \mathbf{C} allows to reformulate the optimization over the integral residual into a quadratic program. Its cost matrix, however, is of size $n(2N_{\mathbf{u}} + 1) \times n(2N_{\mathbf{u}} + 1)$, rendering this criterion inefficient in practice due to the need of numerical quadrature. Alternatively, the residual (13) can be set to zero only at m specific time instants $\{t_1, \dots, t_m\}$. This reduces the quadratic program to a linear equation system with mn^2 equations of the form

$$\hat{\mathbf{c}}_{\text{all}} (\mathbf{l}_{ij}(t_k) - \mathbf{q}_{ij}(t_k)) = 0, \quad (14)$$

where $\mathbf{l}_{ij}, \mathbf{q}_{ij} \in \mathbb{C}^{n(2N_{\mathbf{u}}+1)}$ determine the (ij) -th matrix entries of the first and second summand in (13), respectively, via

$$\hat{\mathbf{c}}_{\text{all}} \mathbf{l}_{ij}(t) = \left(\dot{\mathbf{C}}(t)e^{\mathbf{H}t}\mathbf{W} + \mathbf{C}\mathbf{H}e^{\mathbf{H}t}\mathbf{W} \right)_{ij}, \quad \hat{\mathbf{c}}_{\text{all}} \mathbf{q}_{ij}(t) = (\mathbf{J}(t)\mathbf{C}(t)e^{\mathbf{H}t}\mathbf{W})_{ij}.$$

After separation of $\hat{\mathbf{c}}_{\text{all}}$ and (14) into their real and imaginary parts and consideration of the constraints (12), this leaves a real linear equation system of size $2mn^2 \times 2nN_{\mathbf{u}}$ and the projection matrix created from its least-squares solution will be denoted as \mathbf{C}_{samp} . Usually, m can be chosen rather small (between 1 and 10) as $N_{\mathbf{u}}$ is seldom chosen to be larger than n .

6 Application to a vertically excited multiple pendulum

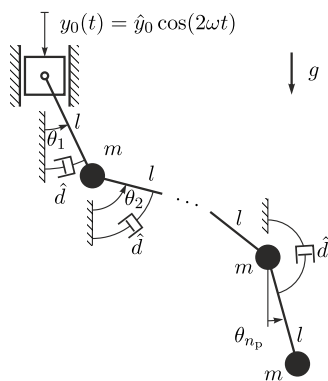
The various considered approaches for the projection matrix \mathbf{C} are illustrated for the linearized dynamics of a vertically excited multiple pendulum. A sketch of the considered mechanical system is given in Figure 2a. The pendulum consists of n_p joints, each of mass m , with viscous absolute damping \hat{d} , linked by n_p rods of length l . The suspension point of the pendulum moves along the direction of gravity with $y_0(t) = \hat{y}_0 \cos(2\omega t)$. The linearized multiple pendulum dynamics

$$\begin{pmatrix} \mathbf{I} & \mathbf{0} \\ \mathbf{0} & \mathbf{M} \end{pmatrix} \begin{pmatrix} \dot{\boldsymbol{\theta}} \\ \ddot{\boldsymbol{\theta}} \end{pmatrix} = \begin{pmatrix} \mathbf{0} & \mathbf{I} \\ -[a + 2b \cos(2\omega t)]\mathbf{D} & -d\mathbf{I} \end{pmatrix} \begin{pmatrix} \boldsymbol{\theta} \\ \dot{\boldsymbol{\theta}} \end{pmatrix} \quad (15)$$

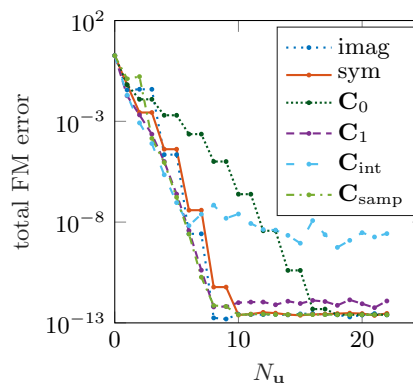
is derived in [7] with the abbreviations

$$(\mathbf{M})_{ij} = n_p + 1 - \max(i, j), \quad \mathbf{D} = \text{diag}(n_p, \dots, 1), \quad a = \frac{g}{l}, \quad b = 2\hat{y}_0 \frac{\omega^2}{l}, \quad d = \frac{\hat{d}}{ml^2}.$$

After inversion of the left matrix, this dynamics is of the form $\dot{\mathbf{y}} = \mathbf{J}(t)\mathbf{y}$ that can be analyzed using the presented methods. For $n_p = 1$, it simplifies to the well-known Mathieu equation.



(a) Sketch of vertically excited multiple pendulum.



(b) Accuracy of Floquet multipliers over N_u for the linearized 1-pendulum with $(a, b, d) = (5, 0.5, 0)$.

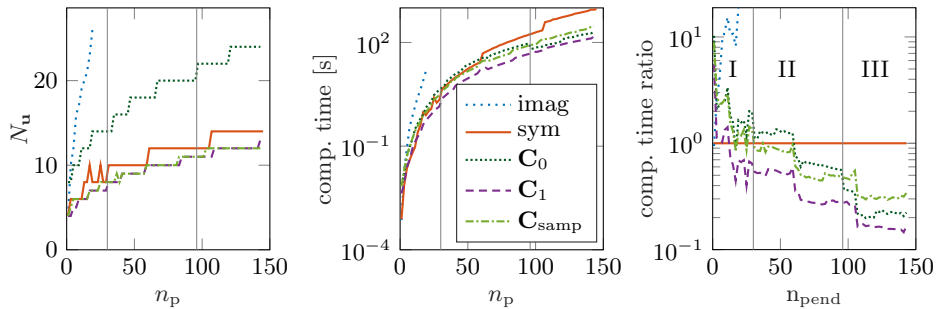
To analyze the convergence behavior of our proposed method, the accuracy of the FM of the equilibrium is studied. As a basis for comparison, the “true” FM are determined from the monodromy matrix obtained by the $2n$ -pass method.

The total FM error $\varepsilon_{\text{total}} = \min_{\pi \in \mathcal{P}} \sqrt{\sum_{l=1}^n |\lambda_{l, \text{true}} - \lambda_{\pi(l), \text{cand}}|^2}$ is defined as the norm of the difference between the “true” FM and the FM candidates obtained by a given method, while the latter are reordered by a permutation $\pi \in \mathcal{P}$ such that this error is minimal.

For $n_p = 1$, i.e. for the Mathieu equation, and parameters $(a, b, d) = (5, 0.5, 0)$, all considered projection matrices \mathbf{C} are compared in Figure 2b. Concerning classical Hill methods, the dotted blue accuracy curve was obtained using the imaginary part sorting criterion [5] and the solid curve with the symmetry-based criterion [3, 11]. The dark green dotted accuracy curve corresponds to the naive projection matrix \mathbf{C}_0 (9). The matrix \mathbf{C}_{samp} was obtained by evaluating (14) for $m = 20$ linearly spaced time instants and its accuracy is given in dashdotted green. The results for the projection matrix \mathbf{C}_{int} , obtained by minimizing the residual in an integral sense, are given in dashed light blue. Noting that the solutions of the quadratic program and the sampled equations have a common structure of alternating entries, the matrix $\mathbf{C}_1 = (\mathbf{I}, -\mathbf{I}, \mathbf{I}, \dots, -\mathbf{I}, \mathbf{I}) \in \mathbb{R}^{n \times N}$ is also included.

All approaches except for the integration-based projection matrix converge towards an accuracy of 10^{-12} , which is the error of the FM obtained by $2n$ -pass. The integration-based projection matrix \mathbf{C}_{int} provides the best estimate for low $N_{\mathbf{u}}$, but as $N_{\mathbf{u}}$ increases and other projection matrices also yield almost-perfect results, rank loss coupled with numerical quadrature inaccuracies prevent a true minimizer with good performance from being found. For this reason, the integration-based approach will not be plotted in the figures below. The error of the Floquet multipliers obtained by the naive choice \mathbf{C}_0 does eventually converge towards (numerically) zero, albeit slower than the other more problem-specific projection matrices. With a similar argument as in [3], as the Hill matrix \mathbf{H} will have a band structure if $N_{\mathbf{u}}$ is chosen sufficiently large, its middle rows are less impacted by the truncation error. As the naive \mathbf{C} matrix only picks these middle rows, the error will eventually converge.

The sparsity-promoting computational benefits of the projection-based methods take effect for larger system sizes. To illustrate this, the considered methods have been evaluated for multiple values of n_p , in each case increasing $N_{\mathbf{u}}$ until a total FM error of less than 10^{-4} is reached. This critical value of $N_{\mathbf{u}}$ is given in Figure 3a, while the computation time to evaluate stability for that $N_{\mathbf{u}}$ is given in Figure 3b. The computation time includes the construction of \mathbf{H} as well as all steps shown in Figure 1, i.e. the large eigenvalue problem along with the eigenvalue sorting for the classical approaches, and the construction of the matrix \mathbf{C} , the matrix exponential and the small eigenvalue problem for the projection-based approaches. For the optimized matrix \mathbf{C}_{samp} , $m = 8$ linearly spaced time samples were chosen in each step, and the matrix exponential of the last time sample $t_8 = T$ was later re-used for the monodromy matrix. In Figure 3c, the ratio of the computation time of the individual methods against the symmetry-based method are given. This means that a method performs faster than the symmetry-based method for a given n_p if this ratio is < 1 .



(a) $N_{\mathbf{u}}$ needed to achieve (b) Computation time (c) Ratio of computation
 FM error $\leq 10^{-4}$. needed for $N_{\mathbf{u}}$ of Fig. 3a. time against sym.-sorting

Fig. 3: $N_{\mathbf{u}}$ and computation time needed to yield FM estimates with an accuracy better than 10^{-4} for varying n_p and parameters $(a, b, d) = (5, 0.5, 0)$.

The imaginary-part based method only identifies the correct FM candidates for very large $N_{\mathbf{u}}$, incurring exorbitant and not practically feasible computation times. In contrast, the symmetry-based sorting criterion is able to identify the correct FM candidates already for rather small $N_{\mathbf{u}}$ for all considered values of n_p , confirming the qualitative behavior reported in [11]. While the problem-specific projection matrices \mathbf{C}_1 and \mathbf{C}_{samp} need similar values of $N_{\mathbf{u}}$ as the symmetry-based criterion, the naive projection matrix \mathbf{C}_0 only converges for larger $N_{\mathbf{u}}$. In the computation time diagram 3b, this yields multiple break-even points between the individual approaches, separating the n_p space into three regions. In region I, for small n_p , the computational overhead of all projection-based methods is large since more steps of similar matrix size have to be performed than in the classical approaches. In region II starting at $n_p = 30$, however, the optimized projection matrix \mathbf{C}_{samp} is faster than the classical symmetry-based method as solving the large eigenvalue problem becomes more costly while the computational effort of the matrix exponential grows with a more gentle slope. The onset of region III is characterized by the break-even point of the optimized matrix \mathbf{C}_{samp} and the naive matrix \mathbf{C}_0 . In this region, the effort of evaluating the matrix exponential at $m - 1$ additional time instants and solving a system of mn^2 linear equations is more costly than increasing $N_{\mathbf{u}}$. The matrix \mathbf{C}_1 has the least computational effort in all approaches, but as it was determined by manual inspection, the behavior of the projection matrix \mathbf{C}_1 can not be extended to systems beyond the considered multiple pendulum.

7 Conclusion

The numerical experiments reported in Section 6 have shown that the projection matrix \mathbf{C} in the newly introduced projection-based Hill method greatly influences accuracy and convergence speed of the proposed method. Various ways of identifying a suitable projection matrix differing in theoretical and computational effort have been compared. While the naive projection matrix \mathbf{C}_0 always converges towards the correct values, the convergence rate w.r.t the frequency order $N_{\mathbf{u}}$ can be improved for other choices. In particular, the evaluation of the approximated LTV dynamics over one period using few time samples yields a projection matrix estimate that improves this performance. However, this again incurs additional numerical effort.

The tradeoff between solving the large eigenvalue problem of the classical methods, solving a system of linear equations for an optimized \mathbf{C} matrix and needing larger $N_{\mathbf{u}}$ for the same accuracy range divides the space of system orders into multiple regions. While the projection-based method can not compete effort-wise against the state-of-the-art symmetry-based Hill method for small system sizes, for high numbers of DOF, as they do usually occur in practice, this method offers significant benefits regarding computational cost. For the multiple pendulum, the optimization using additional time samples can also be used with a low frequency order $N_{\mathbf{u}}$, and hence low numerical effort, to identify structure

in the optimal \mathbf{C} matrix, which can then explicitly be used for larger but similar systems with even smaller computational effort.

Beyond the mainly academical examples in this work, it would be expedient to apply the novel stability method to systems of more practical relevance. Large systems that were already analyzed extensively using the MANLAB framework (e.g. [12]) could benefit from the stability insights of our proposed method, while simultaneously serving as practical examples of the performance of the method.

References

1. Krack, M., Gross, J.: *Harmonic Balance for Nonlinear Vibration Problems*. Springer, Cham (2019)
2. Detroux, T., Renson, L., Masset, L., Kerschen, G.: The harmonic balance method for bifurcation analysis of large-scale nonlinear mechanical systems. *Computer Methods in Applied Mechanics and Engineering* 296, 18–38 (2015)
3. Lazarus, A., Thomas, O.: A harmonic-based method for computing the stability of periodic solutions of dynamical systems. *Comptes Rendus Mécanique* 338(9), 510–517 (2010)
4. Peletan, L., Baguet, S., Torkhani, M., Jacquet-Richardet, G.: A comparison of stability computational methods for periodic solution of nonlinear problems with application to rotordynamics. *Nonlinear Dynamics* 72(3), 671–682 (2013)
5. Zhou, J., Hagiwara, T., Araki, M.: Spectral characteristics and eigenvalues computation of the harmonic state operators in continuous-time periodic systems. *Systems & Control Letters* 53(2), 141–155 (2004)
6. Wu, J., Hong, L., Jiang, J.: A robust and efficient stability analysis of periodic solutions based on harmonic balance method and Floquet-Hill formulation. *Mechanical Systems and Signal Processing* 173, 109057 (2022), <https://www.sciencedirect.com/science/article/pii/S0888327022002291>
7. Bayer, F., Leine, R.I.: Sorting-free Hill-based stability analysis of periodic solutions through Koopman analysis. *ResearchSquare* [Preprint], submitted for publication (2022), <https://www.researchsquare.com/article/rs-2183060/v1>
8. Teschl, G.: *Ordinary Differential Equations and Dynamical Systems*. No. 140 in *Graduate Studies in Mathematics*, American Mathematical Society, Providence, Rhode Island (2012)
9. Mauroy, A., Mezić, I., Susuki, Y. (eds.): *The Koopman Operator in Systems and Control. Concepts, Methodologies and Applications*. No. 484 in *Lecture Notes in Control and Information Sciences*, Springer, Cham (2020)
10. Al-Mohy, A.H., Higham, N.J.: Computing the action of the matrix exponential, with an application to exponential integrators. *SIAM Journal on Scientific Computing* 33(2), 488–511 (2011)
11. Guillot, L., Lazarus, A., Thomas, O., Vergez, C., Cochelin, B.: A purely frequency based Floquet-Hill formulation for the efficient stability computation of periodic solutions of ordinary differential systems. *Journal of Computational Physics* 416, 109477 (2020)
12. Debeurre, M., Grolet, A., Mattei, P.O., Cochelin, B., Thomas, O.: Nonlinear modes of cantilever beams at extreme amplitudes: Numerical computation and experiments. In: Brake, M.R.W., Renson, L., Kuether, R.J., Tiso, P. (eds.) *Nonlinear Structures & Systems*, Volume 1. pp. 245–248. Springer International Publishing, Cham (2023)